

Shot noise in ferromagnetic single electron tunneling devices

B.R. Bulka¹, J. Martinek¹, G. Michalek¹ and J. Barnaś²

¹*Institute of Molecular Physics, Polish Academy of Sciences,
ul. Smoluchowskiego 17, 60-179 Poznań, Poland*

²*Department of Physics, A. Mickiewicz University,
ul. Umultowska 85, 61-614 Poznań, Poland*

(February 26, 2018)

Frequency dependent current noise in ferromagnetic double junctions with Coulomb blockade is studied theoretically in the limit of sequential tunneling. Two different relaxation processes are found in the correlations between spin polarized tunneling currents; low frequency spin fluctuations and high frequency charge fluctuations. Spin accumulation in strongly asymmetric junctions is shown to lead to a negative differential resistance. We also show that large spin noise activated in the range of negative differential resistance gives rise to a significant enhancement of the current noise.

75.70.Pa, 73.50.Td, 73.23.Hk, 73.40.Gk

I. INTRODUCTION

Recent progress in nanotechnology of magnetic materials renewed interest in spin-polarized electron tunneling in magnetic junctions. This interest is additionally stimulated by expected applications of magnetic junctions in field sensors, magnetic random access memories (MRAMs), and other microelectronic devices. It is well known since the work of Julliere¹, that the junction resistance depends on its magnetic configuration, and this effect, known also as the tunnel magnetoresistance (TMR), offers the possibility of magnetic control of the tunneling current.

A special kind of tunnel junctions are the double barrier junctions with a small central electrode. The increase in electrostatic energy due to charging this electrode with a single electron can lead to Coulomb blockade of electric current below a certain threshold voltage and to Coulomb steps in I-V characteristics at higher voltages. Such junctions, known as single electron transistors (SETs), were extensively studied in the last decade in the limit of nonmagnetic (metallic or semiconducting) electrodes.² However, it is only very recently when the interplay of charge and spin effects in SETs with ferromagnetic electrodes was studied theoretically and experimentally.³⁻⁶ It has been shown that the charging effects give rise to periodic modulations of the TMR effect with increasing bias voltage. It has been also predicted that cotunneling effects in the Coulomb blockade regime can significantly enhance TMR. When intrinsic spin relaxation time on the central electrode (i.e. spin relaxation due to spin-flip scattering within the electrode) is much longer than injection time (time between successive tunneling events), then a nonequilibrium spin distribution of electrons is driven by the flowing current. The corresponding spin accumulation can lead to new effects, like negative differential resistance (NDR) or inverse TMR effect.

A very important parameter, in view of potential applications of the TMR effect, is the noise to signal ratio. In the case of nonmagnetic SETs this problem was recently extensively studied in the relevant literature.⁷⁻¹⁶ It has been shown that the noise can provide additional information on the electronic structure, transport properties and also on electron-electron interactions. A special issue is the problem of suppression of the zero-frequency shot noise by electron correlations. Negative correlations between current pulses, induced by the Pauli principle, can lead to complete suppression of the shot noise in quantum point contacts or to reduction of the noise to $(1/3)S_{Poisson}$ ($S_{Poisson} = 2eI$) in metallic diffusive conductors.⁷⁻⁹ Theoretical studies of current correlations in the presence of Coulomb blockade in SETs by Korotkov¹⁰, Hershfield et al.¹¹ and others¹² showed that the shot noise is reduced to $(1/2)S_{Poisson}$. These predictions were also confirmed experimentally on quantum point contacts, diffusive conductors, resonant tunneling diodes and SETs.¹³⁻¹⁶

However, the situation if ferromagnetic junctions significantly differs from that in nonmagnetic SETs and to our best knowledge there is neither experimental nor theoretical work published up to now on shot noise in ferromagnetic SETs. As we show in this paper, large spin fluctuations, which occur in ferromagnetic junctions, have a significant influence on the shot noise, particularly at low frequencies. We also show that two different relaxation times (spin and charge) appear in the frequency dependent current noise. Large spin fluctuations also occur in nonmagnetic junctions, but they do not contribute to the current noise. Another important result following from our analysis is the presence of an enhanced shot noise (well above $2eI$) in the NDR range. Similar enhancement was recently observed in resonant tunneling diodes. The NDR is due to spin accumulation, which in turn follows from detailed balance of electrons with opposite spins tunneling to and off the central electrode.

The paper is organized as follows. In Section 2 we describe the formalism which we use for shot noise calculations in ferromagnetic SET's with the central electrode small enough so the effects due to charging and discrete energy levels are important. The formalism is an extension of the formalism used for nonmagnetic SET's by including spin degrees of freedom. In section 3 we analyze the charge-charge and spin-spin correlations as well as the current shot noise in ferromagnetic junctions with a nonmagnetic central electrode. The case when one external electrode is made of a strong ferromagnet while the other electrodes are nonmagnetic is considered in Section 4. Final conclusions and discussion are in section 5.

II. DESCRIPTION OF MODEL AND METHOD OF CALCULATIONS

We consider a double junction in which a nonmagnetic metallic grain is separated from two ferromagnetic leads (source and sink electrodes) by tunnel barriers with the corresponding spin dependent resistances $R_{1\uparrow}$ and $R_{1\downarrow}$ on the right and $R_{2\uparrow}$ and $R_{2\downarrow}$ on the left sides. If the resistances $R_{j\sigma}$ ($j=1,2$) are much larger than the quantum resistance $R_Q = h/2e^2$, electronic transport is dominated by incoherent, sequential tunneling processes and can be described within the orthodox approach,¹⁷ in which tunneling is treated in the lowest-order perturbation theory whereas higher-order tunneling processes (cotunneling) are neglected. To describe tunneling current and shot noise we extend previous descriptions by including the spin degrees of freedom. This generalization is not trivial and leads to effects which are absent in the spinless descriptions.

Electronic transport through the system is governed by the master equation (written in the matrix form)

$$\frac{d\hat{p}}{dt} = \hat{M}\hat{p} \quad (1)$$

for the time evolution of the probability $p(N_\uparrow, N_\downarrow; t)$ to find N_\uparrow and N_\downarrow excess electrons on the grain. In the limit of long intrinsic spin relaxation on the grain (much longer than the time between successive tunneling events) and for spin conserving tunneling processes, the matrix \hat{M} is given by

$$M_{N'_\uparrow N'_\downarrow; N_\uparrow N_\downarrow} = \begin{cases} A(N_\uparrow, N_\downarrow) & \text{for } N'_\uparrow = N_\uparrow \quad \text{and } N'_\downarrow = N_\downarrow, \\ B_\uparrow^\pm(N_\uparrow, N_\downarrow) & \text{for } N'_\uparrow = N_\uparrow \pm 1 \quad \text{and } N'_\downarrow = N_\downarrow, \\ B_\downarrow^\pm(N_\uparrow, N_\downarrow) & \text{for } N'_\uparrow = N_\uparrow \quad \text{and } N'_\downarrow = N_\downarrow \pm 1, \\ 0 & \text{otherwise,} \end{cases} \quad (2)$$

where

$$A(N_\uparrow, N_\downarrow) = -\Gamma_{1\uparrow}^+(N_\uparrow, N_\downarrow) - \Gamma_{1\uparrow}^-(N_\uparrow, N_\downarrow) - \Gamma_{1\downarrow}^+(N_\uparrow, N_\downarrow) - \Gamma_{1\downarrow}^-(N_\uparrow, N_\downarrow) \\ - \Gamma_{2\uparrow}^+(N_\uparrow, N_\downarrow) - \Gamma_{2\uparrow}^-(N_\uparrow, N_\downarrow) - \Gamma_{2\downarrow}^+(N_\uparrow, N_\downarrow) - \Gamma_{2\downarrow}^-(N_\uparrow, N_\downarrow), \quad (3)$$

$$B_\uparrow^\pm(N_\uparrow, N_\downarrow) = \Gamma_{1\uparrow}^\pm(N_\uparrow \pm 1, N_\downarrow) + \Gamma_{2\uparrow}^\pm(N_\uparrow \pm 1, N_\downarrow), \quad (4)$$

$$B_\downarrow^\pm(N_\uparrow, N_\downarrow) = \Gamma_{1\downarrow}^\pm(N_\uparrow, N_\downarrow \pm 1) + \Gamma_{2\downarrow}^\pm(N_\uparrow, N_\downarrow \pm 1). \quad (5)$$

The tunneling rates for electrons with spin σ , tunneling to (+) and off (-) the grain through the j -th junction, are given by¹⁸

$$\Gamma_{j\sigma}^\pm(N_\uparrow, N_\downarrow) = \frac{\Delta E}{e^2 R_{j\sigma}} \sum_i \left[1 + \exp\left(\mp \frac{E_{i\sigma} - \Delta E N_\sigma - E_F}{\frac{1}{2} k_B T}\right) \right]^{-1} \\ \left[1 + \exp\left(\pm \frac{E_{i\sigma} + eV_j(N_\uparrow, N_\downarrow) \mp E_c - E_F}{k_B T}\right) \right]^{-1}, \quad (6)$$

where E_F denotes the Fermi energy and the summation runs over discrete energy levels $E_{i\sigma}$ of the grain, which are assumed to be equally separated with the level spacing ΔE . Apart from this,

$$V_j(N_\uparrow, N_\downarrow) = (-1)^j V \frac{C_1 C_2}{C_j C} + \frac{eN}{C} \quad (7)$$

and $N = N_\uparrow + N_\downarrow$ is the total number of excess electrons on the grain, $C_{1,2}$ are the capacitances of the right of and left junctions, C is the total capacitance $C = C_1 + C_2$, while e and T stand for the electron charge and temperature, respectively. The single-electron charging energy is defined as $E_c = e^2/2C$. When writing Eq.(6) we assumed that

electron energy relaxation time is of the order or shorter than the time between successive tunneling events, so electrons of a given spin orientation are in thermal equilibrium.

The electric current in the stationary state can be calculated from the formula

$$\begin{aligned} I &= e \sum_{N_\uparrow, N_\downarrow} [\Gamma_{1\uparrow}^+(N_\uparrow, N_\downarrow) - \Gamma_{1\uparrow}^-(N_\uparrow, N_\downarrow) + \Gamma_{1\downarrow}^+(N_\uparrow, N_\downarrow) - \Gamma_{1\downarrow}^-(N_\uparrow, N_\downarrow)] p^0(N_\uparrow, N_\downarrow) \\ &= e \sum_{N_\uparrow, N_\downarrow} [\Gamma_{2\uparrow}^-(N_\uparrow, N_\downarrow) - \Gamma_{2\uparrow}^+(N_\uparrow, N_\downarrow) + \Gamma_{2\downarrow}^-(N_\uparrow, N_\downarrow) - \Gamma_{2\downarrow}^+(N_\uparrow, N_\downarrow)] p^0(N_\uparrow, N_\downarrow), \end{aligned} \quad (8)$$

where the probability $p^0(N_\uparrow, N_\downarrow)$ is a solution of the equation $\hat{0} = \hat{M}\hat{p}^0$. One can also determine the average value of any physical quantity X in the stationary state as

$$\langle X \rangle = \sum_{N_\uparrow, N_\downarrow} X_{N_\uparrow, N_\downarrow} p^0(N_\uparrow, N_\downarrow), \quad (9)$$

where $X_{N_\uparrow, N_\downarrow}$ is the representation of X in the space of states described by the numbers N_\uparrow and N_\downarrow of excess electrons on the grain.

To analyze fluctuations in the system we extend the generation-recombination approach¹⁹ for multi-electron channels by generalization of the method developed for spinless electrons in SET¹⁰⁻¹². The time correlation function of the quantities X and Y is expressed as¹⁹

$$\langle X(t)Y(0) \rangle = \sum_{N'_\uparrow, N'_\downarrow; N_\uparrow, N_\downarrow} X_{N'_\uparrow, N'_\downarrow} P(N'_\uparrow, N'_\downarrow; t | N_\uparrow, N_\downarrow; 0) Y_{N_\uparrow, N_\downarrow} p^0(N_\uparrow, N_\downarrow). \quad (10)$$

Here, $P(N'_\uparrow, N'_\downarrow; t | N_\uparrow, N_\downarrow; 0)$ is the conditional probability to find the system in the final state with N'_\uparrow and N'_\downarrow excess electrons at time t , if there was N_\uparrow and N_\downarrow excess electrons in the initial time $t=0$. This probability is determined from the equation

$$\frac{d\hat{P}}{dt} = \hat{M}\hat{P}. \quad (11)$$

In calculations of the current-current correlation functions one has to include the self-correlation terms as well.^{11,10} According to this procedure the Fourier transform of the charge-charge S_{NN} (upper sign) and spin-spin S_{MM} (lower sign) correlation functions are given by

$$S_{NN(MM)}(\omega) = 4 \sum_{N'_\uparrow, N'_\downarrow; N_\uparrow, N_\downarrow} (N'_\uparrow \pm N'_\downarrow) \text{Re} \left[\frac{1}{i\omega \hat{1} - \hat{M}} \right]_{N'_\uparrow, N'_\downarrow; N_\uparrow, N_\downarrow} (N_\uparrow \pm N_\downarrow) p^0(N_\uparrow, N_\downarrow), \quad (12)$$

while the current-current correlation function is

$$S_{II}(\omega) = S_{II}^{Sh} + S_{II}^c(\omega), \quad (13)$$

where the Schottky value (the frequency independent part) is

$$S_{II}^{Sh} = \frac{2e^2}{C^2} \sum_j \left(\frac{C_1 C_2}{C_j} \right)^2 \sum_{N_\uparrow, N_\downarrow} \left[\Gamma_{j\uparrow}^+(N_\uparrow, N_\downarrow) + \Gamma_{j\uparrow}^-(N_\uparrow, N_\downarrow) + \Gamma_{j\downarrow}^+(N_\uparrow, N_\downarrow) + \Gamma_{j\downarrow}^-(N_\uparrow, N_\downarrow) \right] p^0(N_\uparrow, N_\downarrow) \quad (14)$$

and the second term in Eq.(13) is given by

$$\begin{aligned} S_{II}^c(\omega) &= \frac{4e^2}{C^2} \sum_{N'_\uparrow, N'_\downarrow; N_\uparrow, N_\downarrow} \{ C_2 \left[\Gamma_{1\uparrow}^+(N'_\uparrow, N'_\downarrow) - \Gamma_{1\uparrow}^-(N'_\uparrow, N'_\downarrow) + \Gamma_{1\downarrow}^+(N'_\uparrow, N'_\downarrow) - \Gamma_{1\downarrow}^-(N'_\uparrow, N'_\downarrow) \right] \\ &\quad + C_1 \left[\Gamma_{2\uparrow}^-(N'_\uparrow, N'_\downarrow) - \Gamma_{2\uparrow}^+(N'_\uparrow, N'_\downarrow) + \Gamma_{2\downarrow}^-(N'_\uparrow, N'_\downarrow) - \Gamma_{2\downarrow}^+(N'_\uparrow, N'_\downarrow) \right] \} \\ &\quad \times \text{Re} \left[\frac{1}{i\omega \hat{1} - \hat{M}} \right]_{N'_\uparrow, N'_\downarrow; N_\uparrow, N_\downarrow} \times \end{aligned}$$

$$\begin{aligned}
& \left\{ \left[C_2 \Gamma_{1\uparrow}^+(N_\uparrow - 1, N_\downarrow) - C_1 \Gamma_{2\uparrow}^+(N_\uparrow - 1, N_\downarrow) \right] p^0(N_\uparrow - 1, N_\downarrow) \right. \\
& + \left[C_2 \Gamma_{1\downarrow}^+(N_\uparrow, N_\downarrow - 1) - C_1 \Gamma_{2\downarrow}^+(N_\uparrow, N_\downarrow - 1) \right] p^0(N_\uparrow, N_\downarrow - 1) \\
& - \left[C_2 \Gamma_{1\uparrow}^-(N_\uparrow + 1, N_\downarrow) - C_1 \Gamma_{2\uparrow}^-(N_\uparrow + 1, N_\downarrow) \right] p^0(N_\uparrow + 1, N_\downarrow) \\
& \left. - \left[C_2 \Gamma_{1\downarrow}^-(N_\uparrow, N_\downarrow + 1) - C_1 \Gamma_{2\downarrow}^-(N_\uparrow, N_\downarrow + 1) \right] p^0(N_\uparrow, N_\downarrow + 1) \right\}. \tag{15}
\end{aligned}$$

In the present case the Green's function $\hat{G}(\omega) = [i\omega\hat{1} - \hat{M}]^{-1}$ is defined in the two-dimensional space of states $(N_\uparrow, N_\downarrow)$, in contrast to the previous approaches for the spinless SETs¹⁰⁻¹², where the corresponding Green's function was in the one-dimensional space (i.e. it was tridiagonal).

III. FLUCTUATIONS AND NOISE IN F-N-F JUNCTIONS

Let us begin our discussion with a nonmagnetic grain connected to two ferromagnetic leads (F-N-F junction). In Fig.1a the current-voltage characteristics are presented for the antiparallel and the parallel configurations. We assumed there the charging energy E_c equal to 10.1meV and the level spacing ΔE equal to 3meV. This means that for the electronic bandwidth $W \approx 10eV$ the metallic grain contains $N_a \sim 10^3-10^4$ atoms ($\Delta E \approx W/N_a$). The temperature $T = 2.3K$ is small enough to see the effects due to discrete charging and discrete structure of the energy levels ($k_B T \ll E_c, \Delta E$). In Fig.1b the charge and spin accumulated on the grain are shown as a function of the bias voltage. The steps in the charge accumulation are related to the steps of the current as they both are caused by discrete charging effects. As the charge accumulation is similar in both configurations, the spin accumulation only occurs for the antiparallel configuration and is absent in the parallel one. This is because we assumed that the ferromagnetic electrodes are made of the same materials, so $R_{1\uparrow}/R_{1\downarrow} = R_{2\uparrow}/R_{2\downarrow}$ in the parallel configuration. The oscillations of the spin accumulation are due to periodic blockade of the channels for electrons with the spin $\sigma = \uparrow$ and $\sigma = \downarrow$. With increasing V the mutual balance between the currents through both junctions leads to an increase in the spin accumulation and this gives rise to shifts of the chemical potentials for electrons with opposite spins. When V increases further, a new channel for spin $\sigma = \downarrow$ opens (in the present case at $V \approx 28mV$), which leads to a decrease of the spin accumulation as the charge accumulation is almost constant. At $V \approx 40mV$ a new channel for electrons with $\sigma = \uparrow$ opens as well and now both the spin and charge accumulations increase and the next cycle begins. Small steps in the curves shown in Fig.1 (and also in the following numerical results) is due to discrete structure of the grain energy levels.

A. Charge and spin fluctuations

In order to study the frequency dependence of the correlation functions $S_{NN}(\omega)$, $S_{MM}(\omega)$ and $S_{II}(\omega)$ we perform their spectral decomposition. Accordingly, we express the correlation functions as the sum

$$S_{XX}(\omega) = 4 \sum_{\lambda < 0} \frac{-\lambda}{\lambda^2 + \omega^2} S_{XX}(\lambda) \tag{16}$$

of the components $S_{XX}(\lambda)$ in the representation of the eigenvalues λ of the matrix \hat{M} . All eigenvalues λ are negative, except the eigenvalue $\lambda = 0$ which corresponds to the stationary solution. The bias dependence of the eigenvalues λ is presented in Fig.2 for the spinless and ferromagnetic SETs (the upper and lower parts, respectively). In the latter case the structure is much more complex than in the former one because the spin degeneracy is removed in ferromagnetic SETs. There is also hybridization of the eigenvalues, especially strong in the low frequency region and for voltages close to the steps in the I - V curves.

Calculations of the noise were performed numerically for the space of states $(N_\uparrow, N_\downarrow)$ dynamically increasing with V , and the convergence of the results was checked for the large space of states, which in an extreme situation included 247 states. The results of the spectral decomposition were compared with those obtained by direct calculation of the Green's function $\hat{G}(\omega)$ for some small values of ω (by inversion of the matrix $[i\omega\hat{1} - \hat{M}]$).¹⁰

An example of the spectral decomposition of the charge-charge, $S_{NN}(\omega)$, and spin-spin, $S_{MM}(\omega)$, correlation functions is shown in Fig.3. The amplitude of the spin noise $S_{MM}(\lambda)$ is two orders of magnitude larger than the amplitude of the charge noise $S_{NN}(\lambda)$. From Fig.3 follows that only a few components are significant; the others are exponentially small and can be omitted. It would be rather difficult to extract experimentally the contributions

corresponding to λ 's, which are close to each other. In such a case one can approximate $S_{NN}(\omega)$ with a single Lorentzian curve by introducing an effective relaxation time,

$$S_{NN}(\omega) = 4 \frac{\tau_{charge}}{1 + \omega^2 \tau_{charge}^2} \text{var}(N), \quad (17)$$

as it would be for poissonian processes of independent tunneling events. Here, $\text{var}(N) = \langle N^2 \rangle - \langle N \rangle^2$ is the variance of N . In Fig.4 we present the characteristics for the charge noise: the variance $\text{var}(N)$ and the inverse of the effective relaxation time $1/\tau_{charge}$. The voltage dependence of $1/\tau_{charge}$ is a periodic function, which has minima at the steps of the charge accumulation and maxima at the points corresponding to the minima of $\text{var}(N)$. The value of $1/\tau_{charge}$ is an order of magnitude larger than the average frequency of electron transfer from the source to sink electrodes, $1/\tau_{tr} = I/e \approx 1\text{GHz}$. This is because the current I is determined by the more resistive junction, for which the electron tunneling frequency is close to $1/\tau_{tr}$, while $1/\tau_{charge}$ ($\sim E_c/\min(R_{j\sigma})$) is determined by the frequency of electron tunneling through the less resistive barrier.

Since we assumed the level spacing $\Delta E < E_c$, we can expect large spin fluctuations ($\text{var}(M)$ larger than $\text{var}(N)$) and a long spin relaxation time ($\tau_{spin} > \tau_{charge}$). The analysis of the spin noise has been performed in a similar way as of the charge noise. The corresponding results presented in Fig.5 show that in the case considered $1/\tau_{spin}$ is 20 times smaller than $1/\tau_{charge}$. Since $1/\tau_{spin} \sim \Delta E/\max(R_{j\sigma})$, its value can be even smaller for a larger number of atoms in the grain ($N_a \approx W/\Delta E$). There are also large differences in $\text{var}(M)$ and $1/\tau_{spin}$ in the antiparallel and parallel configurations. The spin fluctuations are significantly smaller in the antiparallel configuration than in the parallel one. This difference is due to large spin accumulation in the antiparallel configuration, which shrinks the space of available states for the spin fluctuations. The small steps in $\text{var}(M)$ and $1/\tau_{spin}$, clearly seen in Fig.5, particularly in the antiparallel configuration, result from the step-like changes of the spin accumulation on the grain. Using the spectral decomposition procedure we found that the dominant contribution to the spin noise comes from the largest eigenvalue λ_1 . This can be concluded from Fig.5b, where the exact value of $1/\tau_{spin}$ (thick solid and dashed curves) is compared with the contribution corresponding to λ_1 (thin solid and dashed curves).

B. Current noise

The current shot noise has been calculated from the formulas (13)-(15). Figure 6a shows the bias dependence of the zero-frequency current noise $S_{II}(\omega = 0)$. The current noise is always smaller in the antiparallel configuration than in the parallel one. This is because in the presence of spin accumulation the amplitude of fluctuations is smaller for the antiparallel configuration. In Fig.6b $S_{II}(\omega = 0)$ is split into two parts; a frequency independent component S_{II}^{Sh} and a contribution $S_{II}^c(\omega = 0)$ arising from the frequency dependent part of the current noise (see Eq.(13)). The component S_{II}^{Sh} is almost constant $\approx 2eI(C_1^2 + C_2^2)/C^2$ at the plateaux of the $I - V$ curve and increases with opening of new channels. Dynamical correlations between the currents are described by $S_{II}^c(\omega)$. Its value in the limit $\omega \rightarrow 0$ can be positive between the $I - V$ steps and negative when new channels become open. This is evident for the antiparallel configuration at $V \approx 26\text{mV}$ when opening a tunneling channel for electrons with $\sigma = \downarrow$ leads to negative dynamical correlations. This effect is almost compensated by an increase in S_{II}^{Sh} and therefore, one gets only a small reduction of the current noise $S_{II}(\omega = 0)$.

A large peak of S_{II}^{Sh} seen in Fig.6b at the threshold of the Coulomb blockade ($V \approx 14\text{mV}$) occurs in any asymmetrical SET device. It is caused by a rapid increase of a stream of tunneling electrons onto the grain, which appears when the conducting channels open. Since the outgoing channel has larger resistance the charge accumulation increases and part of electrons is pushed back to the source electrode. Frequent tunneling of electrons to and from the grain leads to an enhancement of the charge noise as well as of the current noise (see also Fig.4). The reduction of $S_{II}(\omega = 0)$ at $V \approx 14\text{mV}$ and $V \approx 40\text{mV}$ is the effect of the opening of new current channels at the steps of the $I - V$ curves.

Frequency dependence of the $S_{II}^c(\omega)$ component of the current noise is presented in Fig.7a for different voltages. One can clearly distinguish between two different relaxation processes in the current noise; respectively in the low and high frequency ranges. An interesting case is that for $V = 36\text{mV}$ (and also $V = 42\text{mV}$), where anticorrelations between currents occur in a low frequency limit (with $S_{II}^c < 0$) and correlations for higher frequencies ($S_{II}^c > 0$).

In order to determine the effective relaxation time τ_{II} we have performed a detail analysis of $S_{II}^c(\omega)$ as a function of ω . The shape of $S_{II}^c(\omega)$ suggests that there are only a few relaxation processes with well separated relaxation times τ_{II} . Therefore, one can assume that $S_{II}^c(\omega)$ is a superposition of a few Lorentzian curves. The relaxation time for each process is given by $1/\tau_{II}^2 = 3\omega_0^2$, where ω_0 corresponds to the maximal slope of S_{II}^c and can be determined from $d^2 S_{II}^c/d\omega^2 = 0$. The results are presented in Fig.7b by open circles. One can distinguish two distinct relaxation times, one in the high and another one in the low frequency ranges. In a wide voltage range the corresponding relaxation times are very close to the effective relaxation times for the charge and spin noise (compare with the solid curves in

Fig.7b). Some deviations occur for voltages where new tunneling channels become open. In a certain voltage range there are three relaxation times (e.g. at $V \approx 36\text{mV}$ - see also the curve with squares in Fig.7a). This analysis shows that both charge and spin fluctuations are relevant for the shot noise of the current in ferromagnetic SETs.

C. Paramagnetic limit

An interesting limit of the F-N-F junction discussed above is the case where all electrodes are nonmagnetic. It is important to note that large spin fluctuations are present in such the case as well. Fig.8 shows characteristic frequency dependence of S_{II}^c as well as of S_{NN} and S_{MM} . Although the amplitude of the spin noise is very large (in this case it is four orders of magnitude larger than the charge noise), it is not seen in the current noise. In a nonmagnetic system the tunnel resistances for both spin directions are the same. This implies that the components of the current-current correlation functions obey the relation $S_{I_{j\uparrow}I_{j\uparrow}}^c(\lambda) = S_{I_{j\downarrow}I_{j\downarrow}}^c(\lambda)$. For those eigenvalues λ which correspond to the spin noise we have also $S_{I_{j\uparrow}I_{j\uparrow}}^c(\lambda) = -S_{I_{j\uparrow}I_{j\downarrow}}^c(\lambda) < 0$. This means that the tunneling events with the frequency $1/\tau_{spin}$ are anticorrelated for electrons with the same spin and correlated for electrons with the opposite spin. Therefore, the spin component of the total current noise is completely compensated for each junction in a nonmagnetic SET.

The asymmetry between the tunneling channels for electrons with the opposite spins leads to activation of the spin component in the current noise. We extracted from S_{II}^c the components $S_{II}^{c\ charge}$ and $S_{II}^{c\ spin}$ corresponding to the charge and the spin noise, respectively. Their values in the zero-frequency limit are determined from $S_{II}^{c\ charge}(\omega = 0) = -4 \sum_{\lambda < \lambda_0} S_{II}(\lambda)/\lambda$ and $S_{II}^{c\ spin}(\omega = 0) = -4 \sum_{\lambda_0 < \lambda < 0} S_{II}(\lambda)/\lambda$, where $\lambda_0 = -1/\sqrt{\tau_{charge} \tau_{spin}}$. The results are presented in Fig.9 as a function of the parameter p , where $p_1 = p_2$ with $p_j = (R_{j\uparrow} - R_{j\downarrow})/(R_{j\uparrow} + R_{j\downarrow})$ for $j = 1, 2$. It can be seen that the charge component is almost constant whereas the spin component increases with p and for $p \rightarrow 1$ can be much larger than the charge component.

IV. ENHANCEMENT OF THE NOISE IN F-N-N JUNCTIONS

Let us consider now the electron transport through a nonmagnetic metallic grain connected to a nonmagnetic lead on one side and to a ferromagnetic lead on the other side (F-N-N junction). When the ferromagnetic electrode is a strong ferromagnet with only one spin subband (say for spin $\sigma = \downarrow$) partially filled, then the electrons with $\sigma = \uparrow$ can tunnel onto the grain from the nonmagnetic electrode, but the outgoing $\sigma = \uparrow$ channel from the grain to the ferromagnetic electrode is blocked ($R_{2\uparrow} = \infty$). Such a double junction can be considered as a system of coupled SET (for $\sigma = \downarrow$) and a single electron box (SEB) (for $\sigma = \uparrow$). Nonmagnetic coupled SET-SEB devices were recently analyzed theoretically and it was shown that if the coupling is strong, one can have a negative differential resistance (NDR).^{20,21} Heij et al.²¹ constructed recently the SET-SEB device based on two electrostatically coupled metallic grains, and found NDR indeed. In our case we have only a single grain, but two coupled electron channels. In the I - V curve shown in Fig.10 we see NDR with a sequential drop of the current. With increasing V the number of electrons with $\sigma = \uparrow$ on the grain increases (see the spin accumulation in Fig.10b), which results in an increase of the local chemical potential for $\sigma = \uparrow$ electrons and a drop of the current. The maximum drop of I occurs at the maximum of the spin accumulation (at $V \approx 26\text{mV}$). Opening of the next charge channel ($N \rightarrow N + 1$) for conducting electrons ($\sigma = \downarrow$) reduces the spin accumulation and increases the current. Small steps in the charge and spin accumulations are the effect of opening of spin channels, i.e. for $(N_{\uparrow}, N_{\downarrow}) \rightarrow (N_{\uparrow} \pm 1, N_{\downarrow} \mp 1)$.

The noise in magnetic SET-SEB devices has been analyzed with the same method as before and the results for the charge and spin noise are presented in Fig.11. The magnetic fluctuations increase when a new channel opens and then they drop again with increasing voltage. The peaks in $\text{var}(M)$ correspond to the maxima of the effective relaxation time τ_{spin} (the minima of $1/\tau_{spin}$ shown in Fig.11b). The spin noise has a significant influence on the current noise shown in Fig.12. The large increase of the current noise (much over the value $S_{Poisson}$) takes place for the range of NDR, which occurs for voltages corresponding to large spin fluctuations. We performed the spectral decomposition of the current noise $S_{II}^c(\omega)$. The voltage dependence of the eigenvalues λ did not show any peculiarities in the range of NDR. The spectral weight is, however, shifted to lower frequencies. The frequency dependence of $S_{II}^c(\omega)$, shown in Fig.13, exhibits strong increase of the low frequency contribution for the voltages where NDR occurs. Outside the NDR range the low frequency component of the current noise is minor.

Recently, Iannaccone et al.²² studied resonant tunneling through a double barrier GaAs structure and showed an enhancement of the shot noise in the region of NDR. The NDR effect was due to charge accumulation in the central well (the effect predicted by Ricco and Azbel²³). The enhancement of the shot noise was also observed in resonant tunneling through a double barrier in magnetic field,²⁴ although NDR was a result of changes in electronic structure in high magnetic field (formation of Landau levels). Iannaccone et al.²² analyzed the enhancement of the shot noise

in the framework of the generation-recombination approach^{19,25–27} in terms of the effective generation (g) and the recombination (r) rates and their relaxation times τ_g and τ_r , respectively. Such the approach is equivalent to two channel approximation.^{10–12,28} In the present studies we used the method which takes into account multichannel (and multilevel) tunneling processes and therefore we have insight into the microscopic processes related to the tunneling current and its noise.

V. FINAL REMARKS

In summary, we have performed theoretical analysis of the frequency dependent current shot noise in ferromagnetic tunnel junctions in the limit of sequential tunneling. We showed that apart from charge fluctuations there are also strong spin fluctuations, which influence the current noise. The spin noise is significant at low frequencies, while the charge noise at higher frequencies. We predict that two distinct relaxation times τ_{spin} and τ_{charge} should be seen in frequency measurements of the current noise in magnetic tunnel junctions.

We have also studied the magnetic SET-SEB device. The spin accumulation effect can lead in this case to a negative differential resistance, which occurs only when the spin accumulation increases, i.e., when the chemical potential of the *conducting* electrons increases due to accumulation. Spin fluctuations are then activated, which leads to a strong enhancement of the low frequency component of the current noise.

The numerical results have been calculated at a low temperature ($k_B T \ll E_c, \Delta E$), where all features due to discreteness of the system are clearly seen. We have also performed calculations for higher temperatures. The small steps, corresponding to the opening of the magnetic channels, are washed out when $T \rightarrow \Delta E/k_B$. However, the charge and spin fluctuations, $\text{var}(N)$ and $\text{var}(M)$, and the corresponding relaxation times, τ_{charge} and τ_{spin} , remain almost unchanged. In F-N-F junctions (as in Fig.1) the tunnel magnetoresistance, defined as $TMR = I_P/I_{AP} - 1$ (where I_P and I_{AP} are the currents in the parallel and in the antiparallel configurations), decreases with increasing temperature (see also Ref.[29]). For $T > \Delta E/k_B$, the physical quantities become less dependent on the voltage. The values of $\text{var}(N)$ and $\text{var}(M)$ increase with T , as expected. The charge and spin fluctuations are still well separated in the different frequency ranges. At $T = 34.8\text{K}$ the zero-frequency current noise $S_{II}(\omega = 0) \approx 0.8 S_{Poisson}$. The reduction is due to Coulomb correlations, which are still large as $T < E_c/k_B = 117\text{K}$. The component S_{II}^{Sh} is, however, much larger than $S_{Poisson}$, whereas the frequency dependent part $S_{II}^e(\omega)$ is negative with a large amplitude. Its low and high frequency components, corresponding to the spin and the charge fluctuations, are also well defined.

ACKNOWLEDGMENTS

The paper is supported from the State Committee for Scientific Research Republic of Poland within Grant No. 2 P03B 075 14.

¹ M. Julliere, Phys. Lett. **54A**, 225 (1975).

² H. Grabert and M.H. Devoret, eds., *Single Charge Tunneling*, NATO ASI, Series B, vol. 294, Plenum 1992; L.L. Sohn, L.P.Kouwenhoven and G.Schön, eds., *Mesoscopic Electron Transport*, NATO ASI Series E, vol. 345, Kluwer 1997; T. Dittrich, P. Hänggi, G.-L. Ingold, B. Kramer, G. Schü and W. Zwirger, eds., *Quantum Transport and Dissipation*, Wiley-VCH Verlag, 1998, chap.3.

³ K. Ono, H. Shimada, S. Kobayashi and Y. Ootuka, J. Phys. Soc. Jpn. **65**, 3449 (1996); K. Ono, H. Shimada and Y. Ootuka, *ibid.* **66**, 1261 (1997); H. Shimada, K. Ono and Y. Ootuka, J. Phys. Soc. Jpn. **67**, 1359 (1998); H. Brückl, G. Reiss, H. Vitzelberg, M. Bertram, I. Mönch and J. Schumann, Phys. Rev. **B58**, 8893 (1998).

⁴ J. Barnaś and A. Fert, Phys. Rev. Lett. **80**, 1058 (1998).

⁵ S. Takahashi and S. Maekawa, Phys. Rev. Lett. **80**, 1758 (1998); H. Imamura, S. Takashi and S. Maekawa, cond-mat/9809058; F. Guinea, Phys. Rev. **B58**, 9212 (1998).

⁶ J. Barnaś and A. Fert, Europhys. Lett. **44**, 85 (1998); A.N. Korotkov and V.I. Safarov, Phys. Rev. **B59**, 89 (1999); A. Bratas, Yu.V. Nazarov, J. Inoue and G.E.W. Bauer, *ibid.* **B59**, 93 (1999).

⁷ V.A. Khlus, Zh. Eksp. Teor. Fiz. **93**, 2179 (1987); G.B. Lesovik, Pis'ma Zh. Eksp. Teor. Fiz. **49**, 513 (1989).

⁸ M. Buttiker, Phys. Rev. Lett. **65**, 2901 (1990); C.W.J. Beenakker and M. Buttiker, Phys. Rev. **B46**, 1889 (1992).

- ⁹ M.J.M. de Jongh and C.W.J. Beenakker, in *Mesoscopic Electron Transport*, eds. L.L. Sohn, L.P.Kouwenhoven and G.Schön, NATO ASI Series E, vol. 345, Kluwer 1997, p.225; C.W.J. Beenakker, *Rev. Mod. Phys.* **69**, 731 (1997).
- ¹⁰ A.N. Korotkov, *Phys. Rev.* **B49**, 10381 (1994).
- ¹¹ S. Hershfield, J.D. Davies, P. Hyldgaard, C.J. Stanton and J.W. Wilkins, *Phys. Rev.* **B47**, 1967 (1993).
- ¹² U. Hanke, Y. M. Galperin, K. A. Chao and N. Zou, *Phys. Rev.* **B48**, 17209 (1993); U. Hanke, Y. M. Galperin and K. A. Chao and N. Zou, *ibid.* **50**, 1595 (1994); A. Imamoglu and Y. Yamamoto, *Phys. Rev. Lett.* **70**, 3327 (1993).
- ¹³ Y.P. Li, D.C. Tsui, J.J. Heremans, J.A. Simmons and G.W. Weimann, *Appl. Phys. Lett.* **57**, 774 (1990); M. Reznikov, M. Heiblum, H. Shtrikman and D. Mahalu, *Phys. Rev. Lett.* **75**, 3340 (1995).
- ¹⁴ F. Liefink, J.I. Dijkhuis, M.J.M. de Jong, L.W. Molenkamp and H. van Houten, *Phys. Rev.* **B49**, 14 066 (1994); R.J. Schoelkopf, P.J. Burke, A.A. Kozhevnikov, D.E. Prober and M.J. Rooks, *Phys. Rev. Lett.* **78**, 3370 (1997); H.E. van den Brom and J.M. van Ruitenbeck, *ibid.* **82**, 1526 (1999); M. Henny, S. Oberholzer, C. Strunk and C. Schonenberger, *Phys. Rev.* **B59**, 2871 (1999).
- ¹⁵ Y.P. Li, A. Zaslavsky, D.C. Tsui, M. Santos and Shayegan, *Phys. Rev.* **B41**, 8388 (1990); H.C. Liu, J. Li, G.C. Aers, C.R. Leavens, M. Buchmanan and Z.R. Wasilewski, *ibid.* **51**, 5116 (1995).
- ¹⁶ H. Birk, M.J.M. de Jong and C. Schonenberger, *Phys. Rev. Lett.* **75** 1610 (1995).
- ¹⁷ H. Grabert and M.H. Devoret, eds., *Single Charge Tunneling*, NATO Advanced Study Institute, Series B, vol. 294, Plenum 1992; G. Schön, in *Quantum Transport and Dissipation*, eds. T. Dittrich, P. Hänggi, G.-L. Ingold, B. Kramer, G. Schön and W. Zwerger, Wiley-VCH Verlag, 1998, chap.3.
- ¹⁸ C.W.J. Beenakker, *Phys. Rev.* **B44**, 1646 (1991).
- ¹⁹ K.M. van Vliet and J.R. Fassett, in *Fluctuation Phenomena in Solids*, ed. R.E. Burgess, Academic Press 1965, p.267.
- ²⁰ H. Nakashima and K. Uozumi, *Jpn. J. Appl. Phys.* **34**, L1659 (1995); M. Shin, S. Lee, K. W. Park and E-H. Lee, *Phys. Rev. Lett.* **80**, 5774 (1998).
- ²¹ C.P. Heij, D.C. Dixon, P. Hadley and J.E. Mooij, *Appl. Phys. Lett.* **74**, 1042 (1999).
- ²² G. Iannaccone, G. Lombardi, M. Macucci and B. Pellegrini, *Phys. Rev. Lett.* **80**, 1054 (1998).
- ²³ B. Ricco and M.Ya. Azbel, *Phys. Rev.* **B29**, 1970 (1984).
- ²⁴ E.R. Brown, *IEEE Trans. Electron. Devices* **39**, 2686 (1992); V.V. Kuznetsov, E.E. Mendez, J.B. Bruno and J.T. Pham, *Phys. Rev.* **B58**, 10159 (1998).
- ²⁵ J.H. Davies, P. Hyldgaard, P.S. Hershfield and J.W. Wilkins, *Phys. Rev.* **B46**, 9260 (1992).
- ²⁶ G. Iannaccone, M. Macucci and B. Pellegrini, *Phys. Rev.* **B55**, 4539 (1997).
- ²⁷ A. van der Ziel, *Noise in measurements*, John Wiley and Sons, 1974.
- ²⁸ M. Eto, *Jpn J. Appl. Phys.* **36**, 4004 (1997).
- ²⁹ G. Michałek, J.Martinek, J. Barnaś and B.R. Bulka, *Mol. Phys. Rep.* (in press); J.Martinek, J. Barnaś, G. Michałek, B.R. Bulka and A. Fert, cond-mat/9810195.

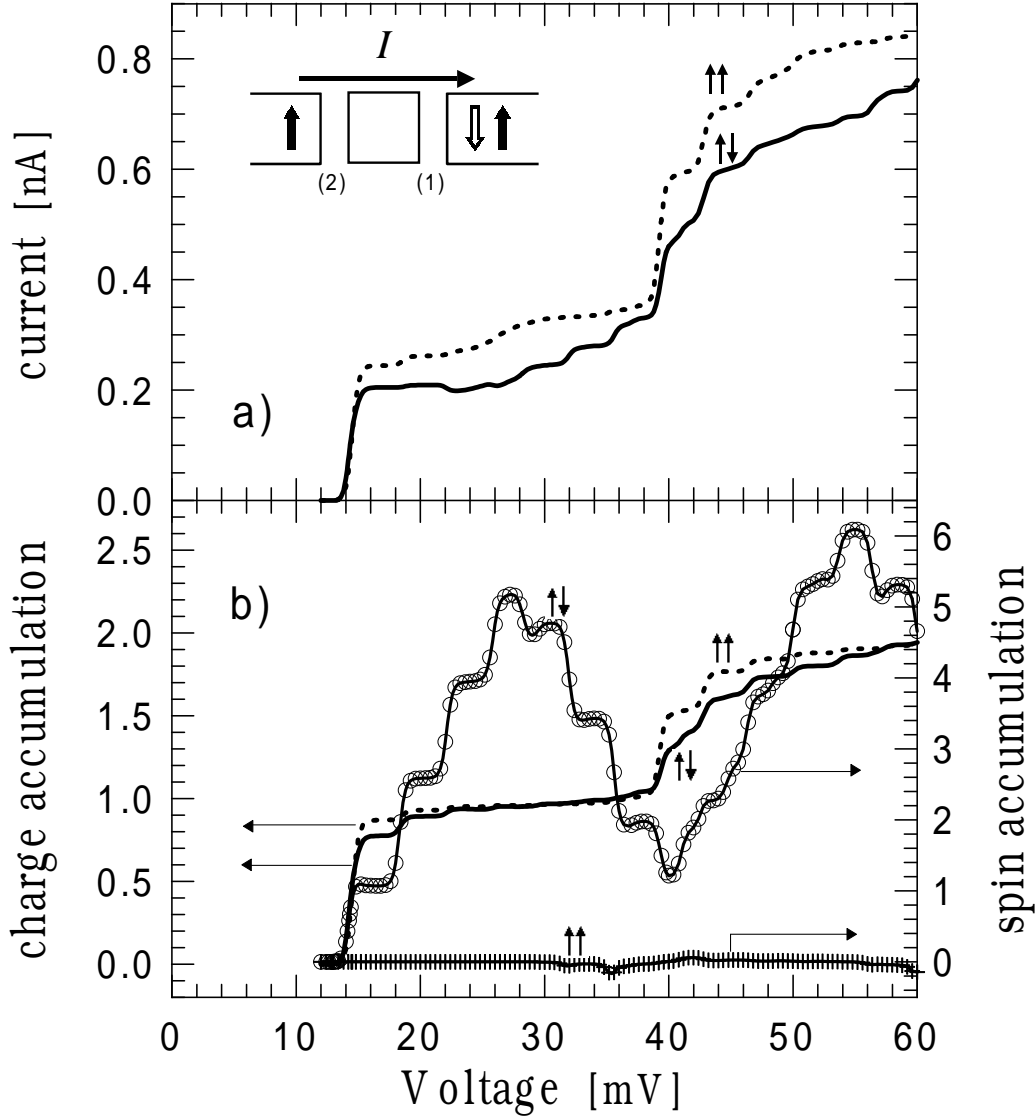


FIG. 1. Voltage dependences of the current (a) and charge (solid and dashed curves) and spin (curves with circles and crosses) accumulation (b) in the antiparallel and the parallel configurations. The parameters assumed here are: $R_{2\uparrow} = 240\text{M}\Omega$, $R_{2\downarrow} = 60\text{M}\Omega$, $R_{1\uparrow} = 2\text{M}\Omega$ and $R_{1\downarrow} = 8\text{M}\Omega$ for the antiparallel configuration ($R_{2\uparrow} = 240\text{M}\Omega$, $R_{2\downarrow} = 60\text{M}\Omega$, $R_{1\uparrow} = 8\text{M}\Omega$ and $R_{1\downarrow} = 2\text{M}\Omega$ for the parallel configuration), $C_2 = 6.6\text{aF}$, $C_1 = 1.32\text{aF}$, $\Delta E = 3\text{meV}$ and $T = 2.3\text{K}$. The inset in part (a) shows the scheme of the system (electrons flow from right to left).

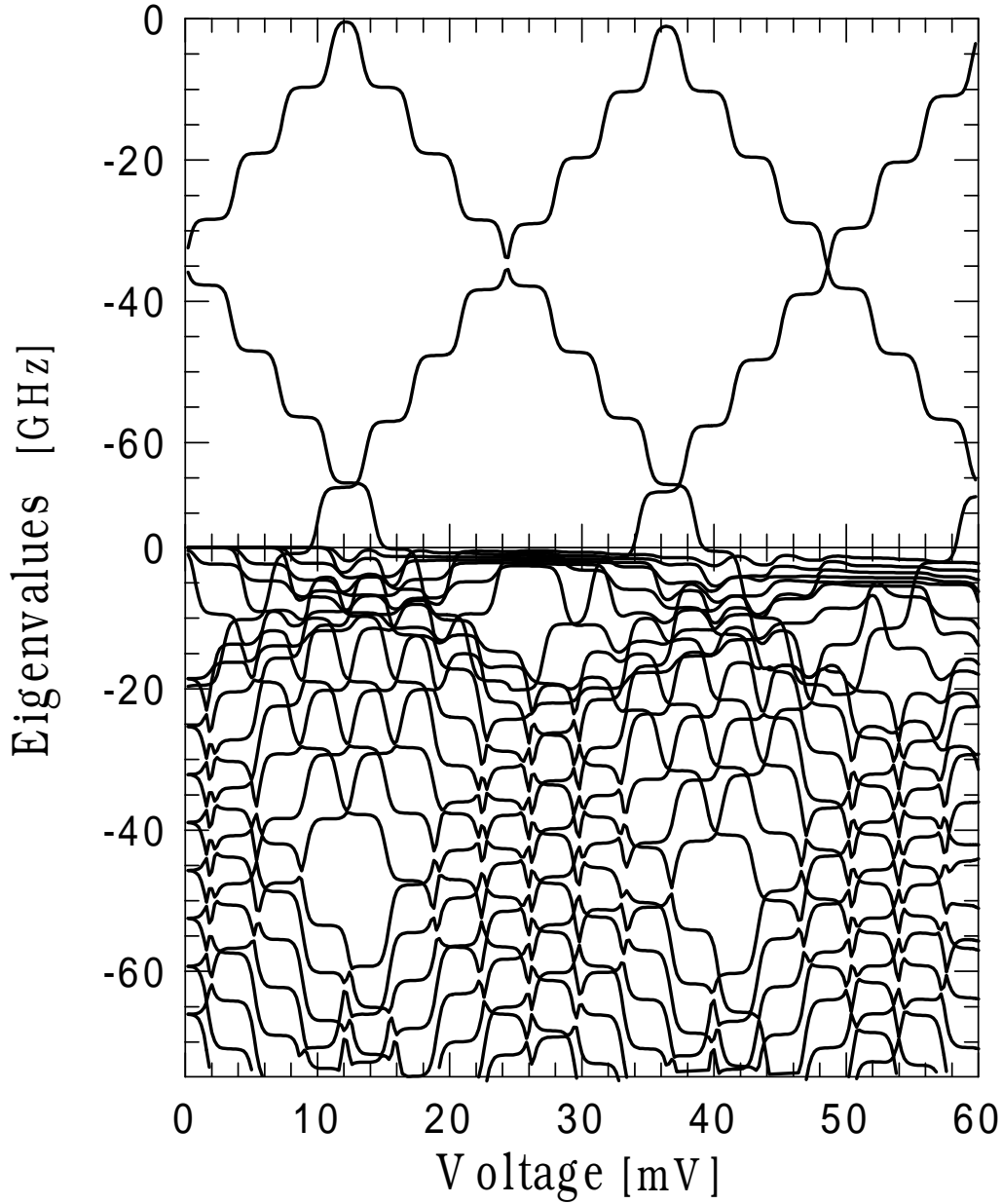


FIG. 2. Voltage dependence of the eigenvalues λ of the matrix \hat{M} for the spinless (the upper part) and ferromagnetic (bottom part) SETs. The parameters assumed in (a) are: $R_2 = 240\text{M}\Omega$, $R_1 = 2\text{M}\Omega$, $C_2 = 6.6\text{aF}$, $C_1 = 1.32\text{aF}$ and $\Delta E = 3\text{meV}$, while in (b) are the same as in Fig.1 for the antiparallel configuration. The space of states is confined to $-5 \leq N \leq 5$ for the spinless SET and $-1 \leq N \leq 4$, $-8 \leq M \leq 8$ for the ferromagnetic SET.

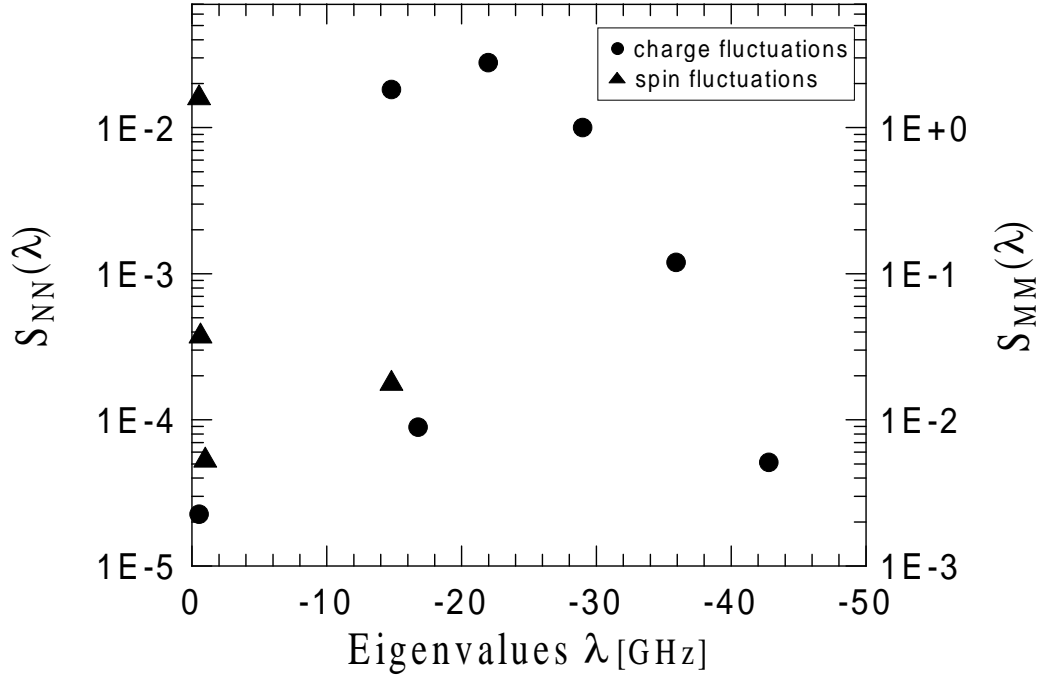


FIG. 3. The components of the spectral decomposition of the charge-charge and the spin-spin correlation functions: $S_{NN}(\lambda)$ (dots) and $S_{MM}(\lambda)$ (triangles), determined for $V = 25\text{mV}$. The other parameters are as in Fig.1 for the antiparallel configuration.

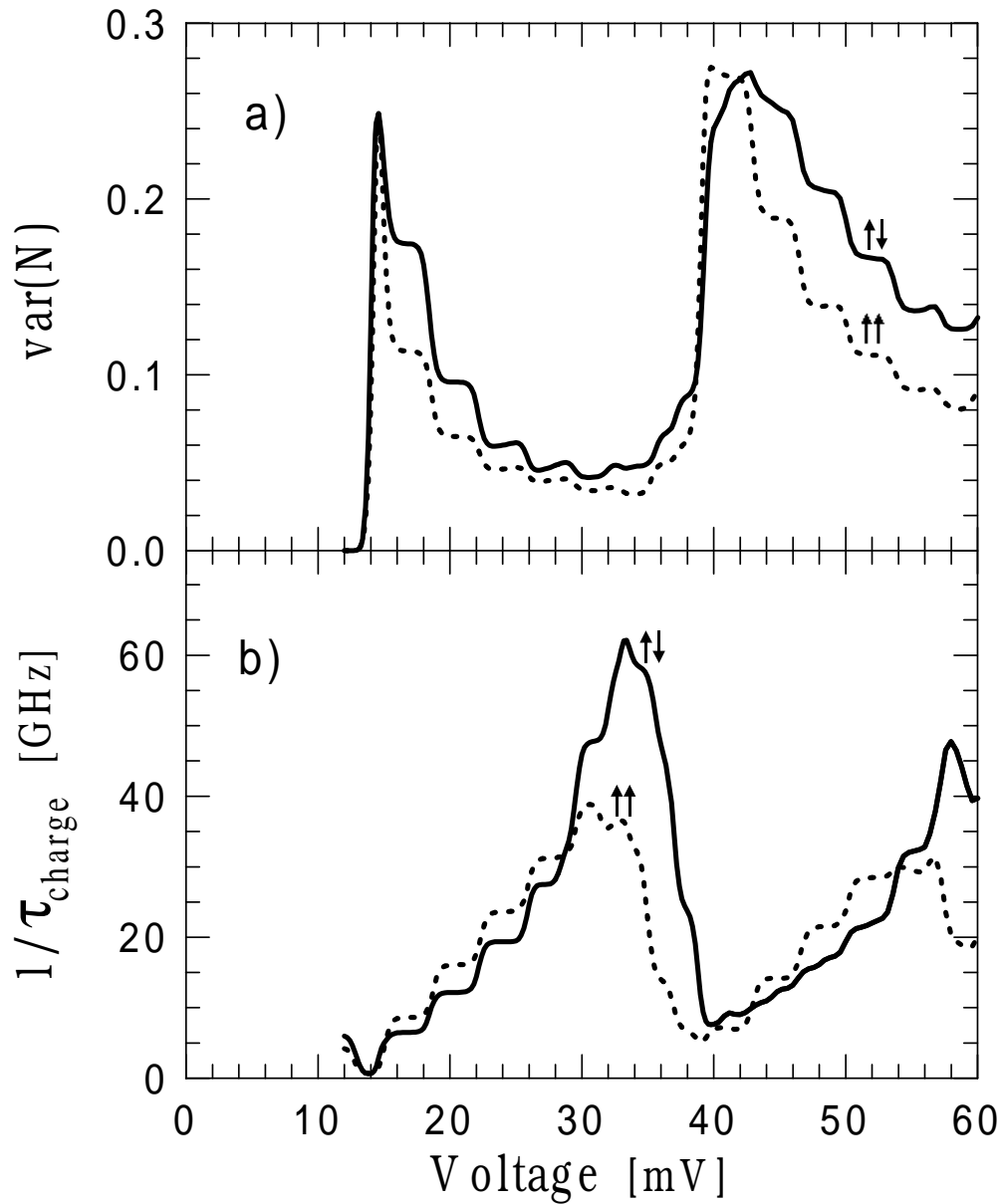


FIG. 4. Voltage dependence of the variance of charge fluctuations, $\text{var}(N)$, (a) and of the inverse effective relaxation time, $1/\tau_{\text{charge}}$, (b) for the parallel and antiparallel configurations. The parameters are the same as in Fig.1.

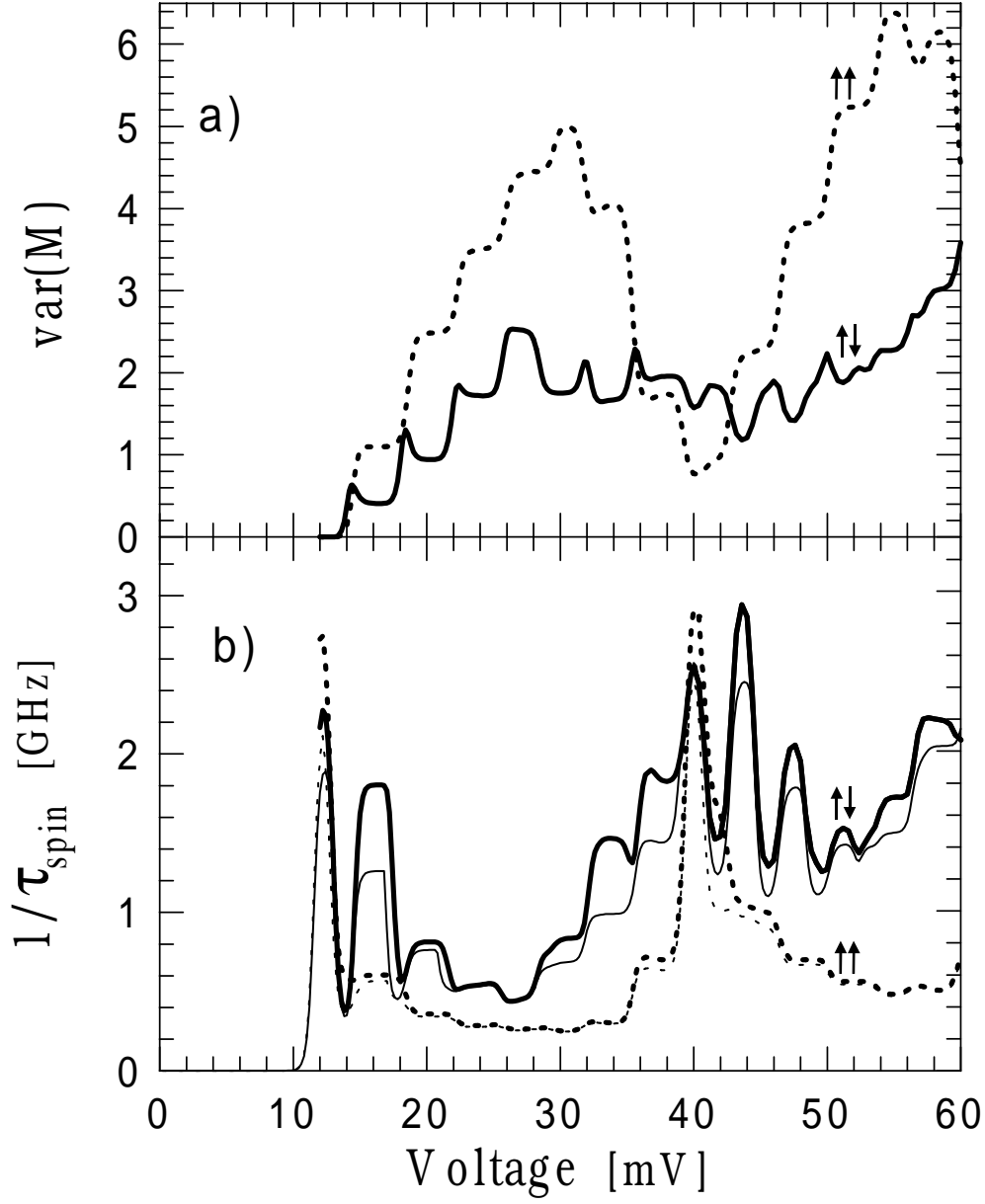


FIG. 5. Voltage dependence of the variance $\text{var}(M)$ of the spin fluctuations (a) and of the inverse effective relaxation time $1/\tau_{\text{spin}}$ (b) in the antiparallel and the parallel configurations. The parameters are the same as in Fig.1. The thin (solid and dashed) curves in part (b) present contribution corresponding to λ_1 , where λ_1 is the largest eigenvalue of the matrix \hat{M} .

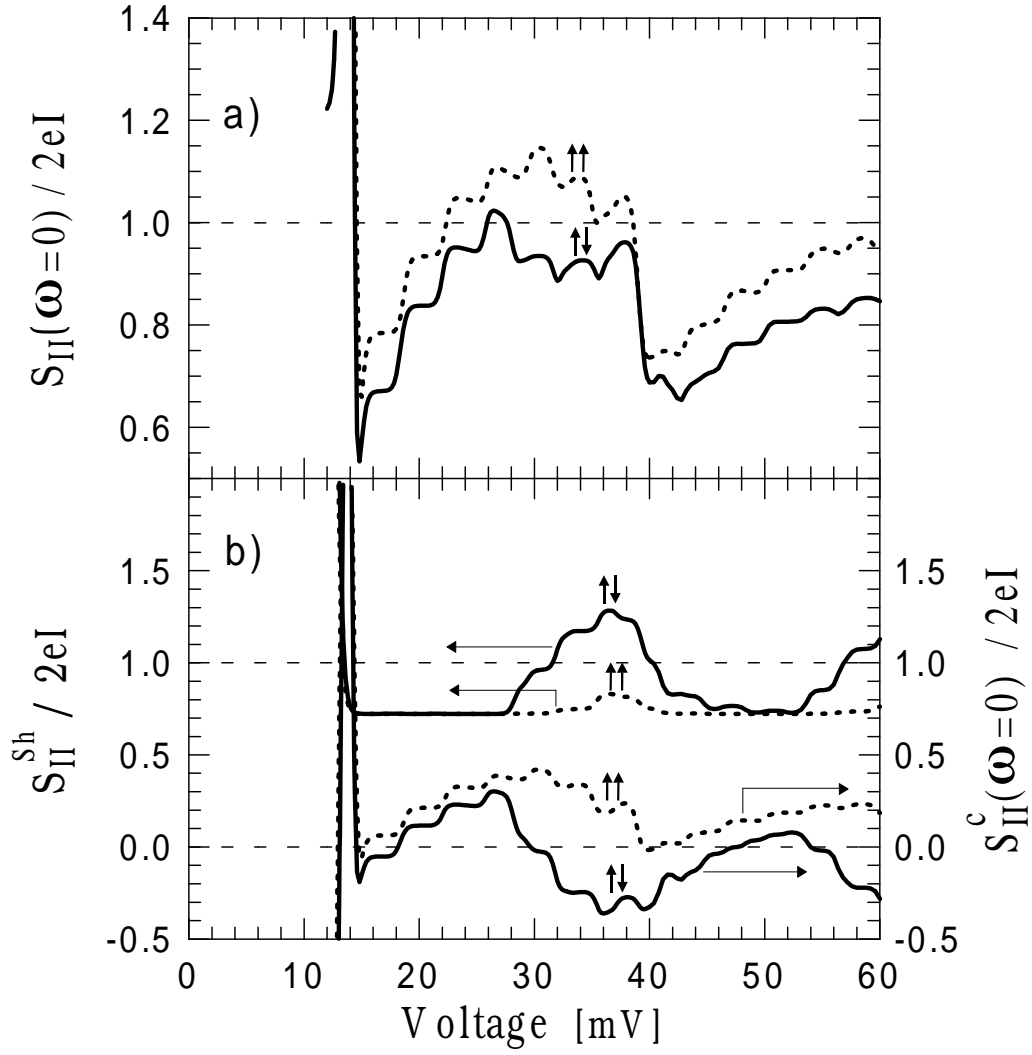


FIG. 6. Voltage dependence of the current shot noise at $\omega = 0$ (a) for the system defined in Fig.1. In part (b) $S_{II}(\omega = 0)$ is split into two components: S_{II}^{sh} (upper curves) and $S_{II}^c(\omega = 0)$ (lower curves).

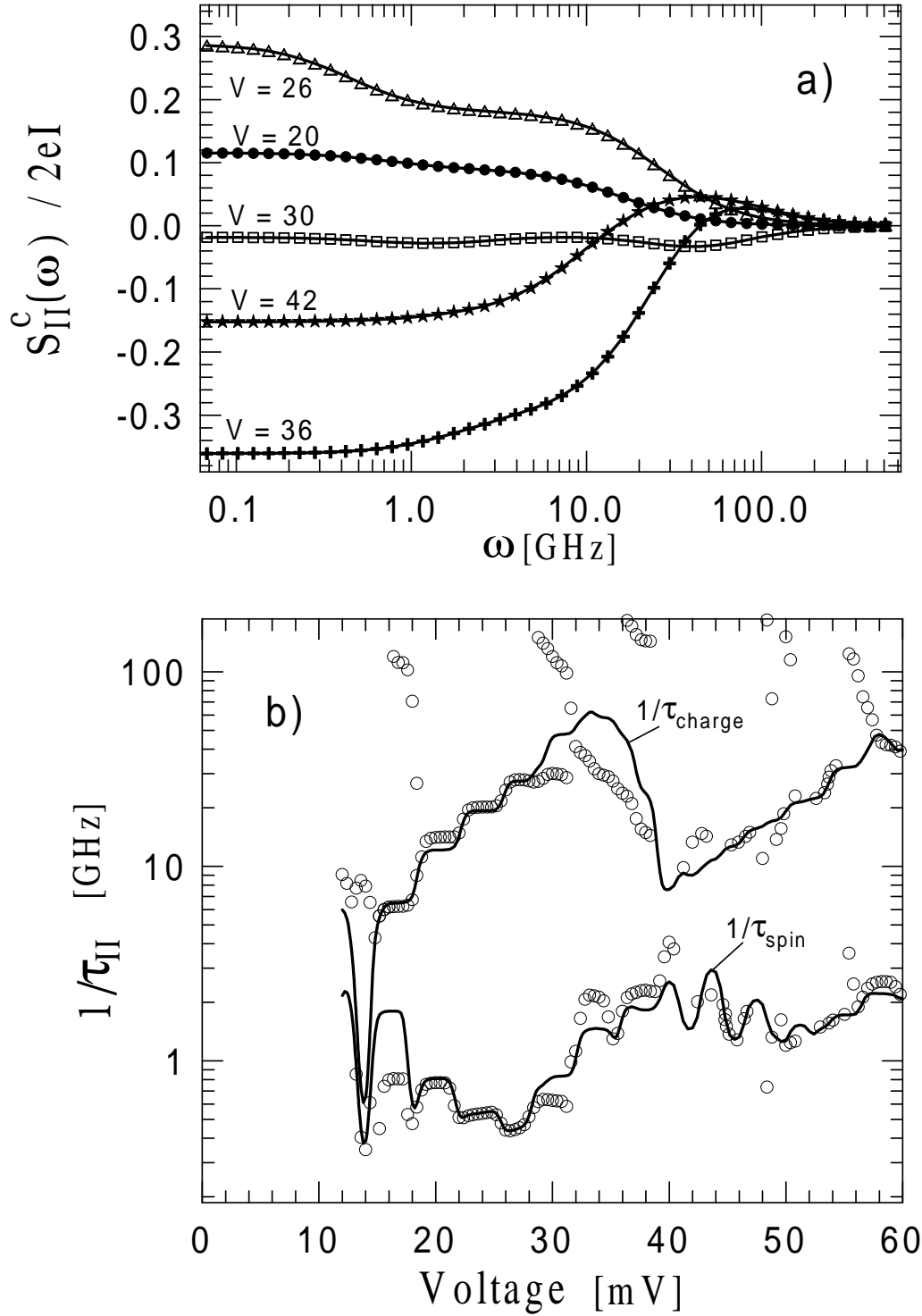


FIG. 7. (a) Frequency dependence of the current shot noise $S_{II}^c(\omega)$ in the system defined in Fig.1 for the antiparallel configuration. (b) Inverse of the relaxation time for the current noise (open circles) as a function of V . For comparison the inverse of the effective relaxation times $1/\tau_{charge}$ and $1/\tau_{spin}$ for the charge and the spin noise are shown by the solid upper and the lower curve, respectively (the same curves as the solid ones in Fig.4b and Fig.5b).

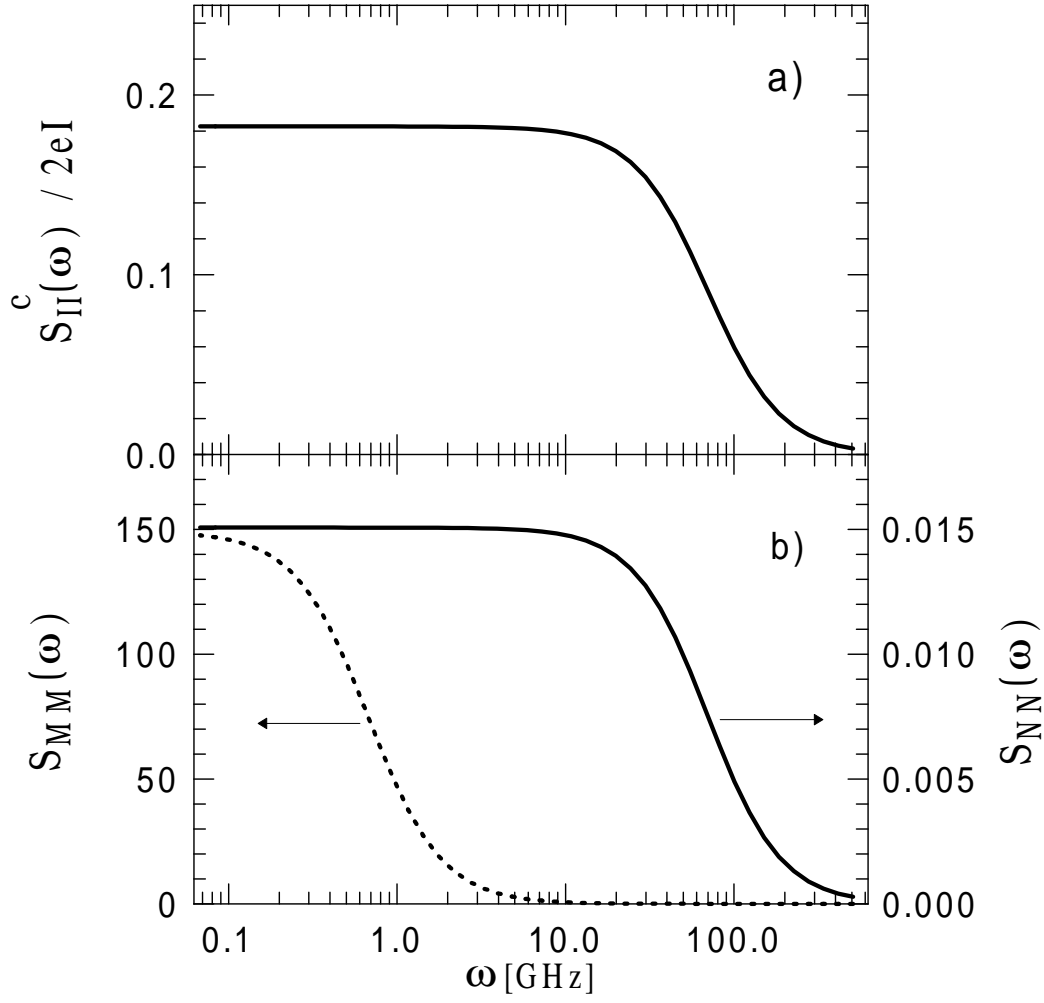


FIG. 8. Frequency dependence of the current noise $S_{II}^c(\omega)$ (a), and of the spin and charge noise (b) at $V = 26\text{mV}$ in a nonmagnetic junction. The parameters assumed are: $R_{1\uparrow} = R_{1\downarrow} = 2\text{M}\Omega$, $R_{2\uparrow} = R_{2\downarrow} = 60\text{M}\Omega$, $C_2 = 6.6\text{aF}$, $C_1 = 1.32\text{aF}$, $\Delta E = 3\text{meV}$ and $T = 2.3\text{K}$.

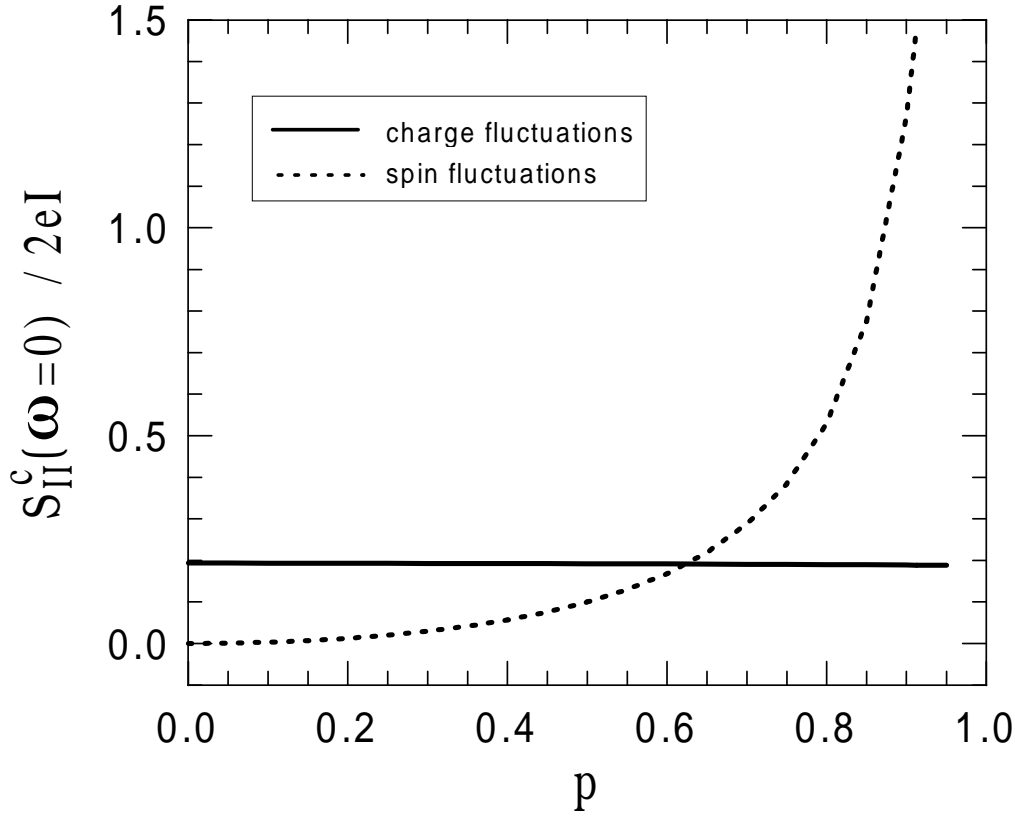


FIG. 9. Two components of $S_{II}^c(\omega = 0)$ corresponding to the charge and spin noise plotted as a function of $p = (R_{1\uparrow} - R_{1\downarrow})/(R_{1\uparrow} + R_{1\downarrow}) = (R_{2\uparrow} - R_{2\downarrow})/(R_{2\uparrow} + R_{2\downarrow})$. The other parameters assumed here are: $R_{2\downarrow} = 60\text{M}\Omega$, $R_{2\uparrow} = (1 + p)/(1 - p)R_{2\downarrow}$, $R_{1\downarrow} = 2\text{M}\Omega$, $R_{1\uparrow} = (1 + p)/(1 - p)R_{1\downarrow}$, $C_2 = 6.6\text{aF}$, $C_1 = 1.32\text{aF}$, $\Delta E = 3\text{meV}$ and $T = 2.3\text{K}$.

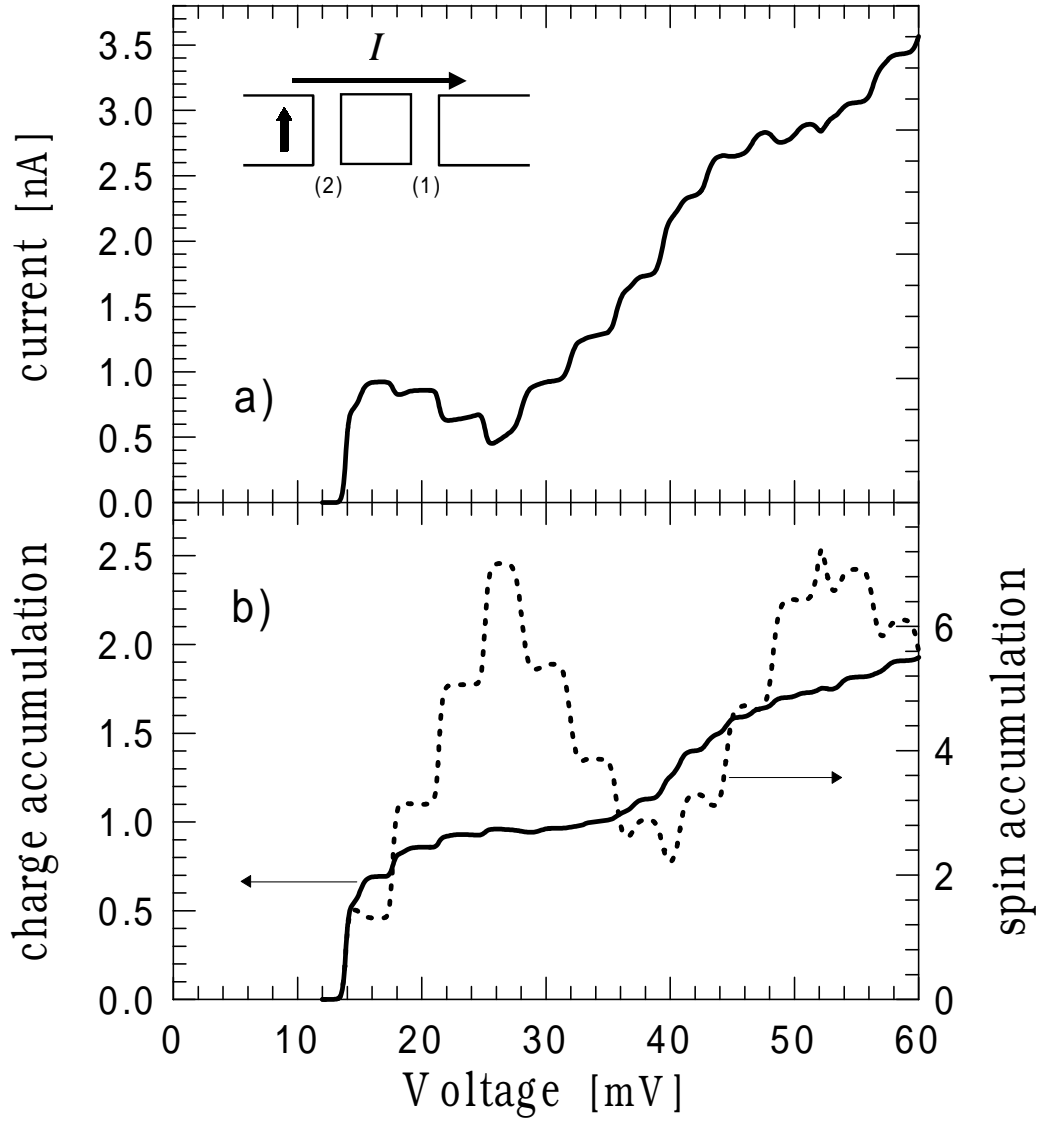


FIG. 10. The $I-V$ curve (a) and the charge and spin accumulation (b) for a F-N-N junction. The parameters assumed are: $R_{2\uparrow} = \infty$, $R_{2\downarrow} = 9M\Omega$, $R_{1\uparrow} = R_{1\downarrow} = 2M\Omega$, $C_2 = 6.6aF$, $C_1 = 1.32aF$, $\Delta E = 3meV$ and $T = 2.3K$. The inset shows the scheme of the system (electrons flow from the nonmagnetic to the ferromagnetic electrode).

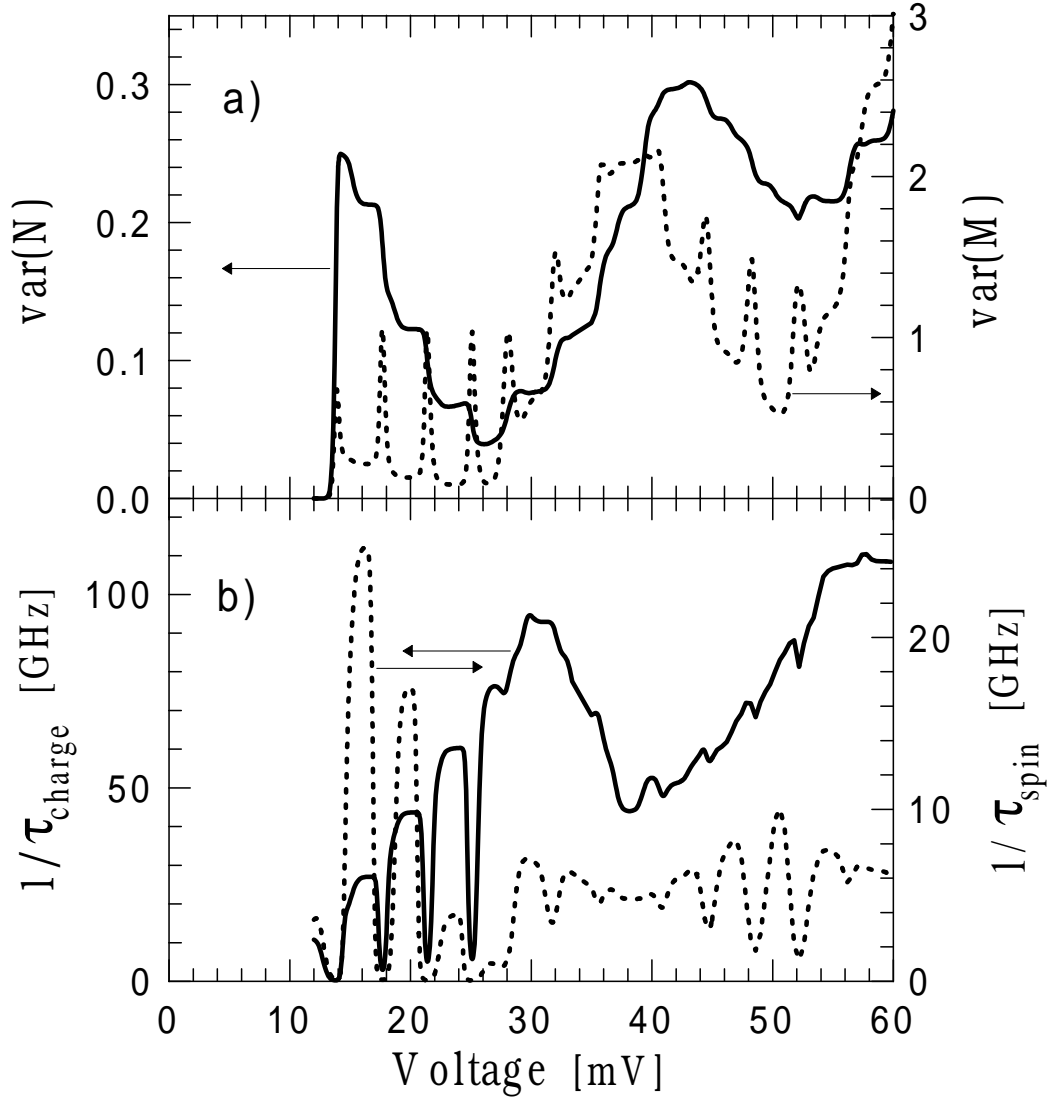


FIG. 11. The variance of the charge and spin fluctuations (a) and the inverse effective relaxation times $1/\tau_{\text{charge}}$ (solid curve) and $1/\tau_{\text{spin}}$ (dashed curve) (b) as a function of the bias voltage for the system as in Fig.10.

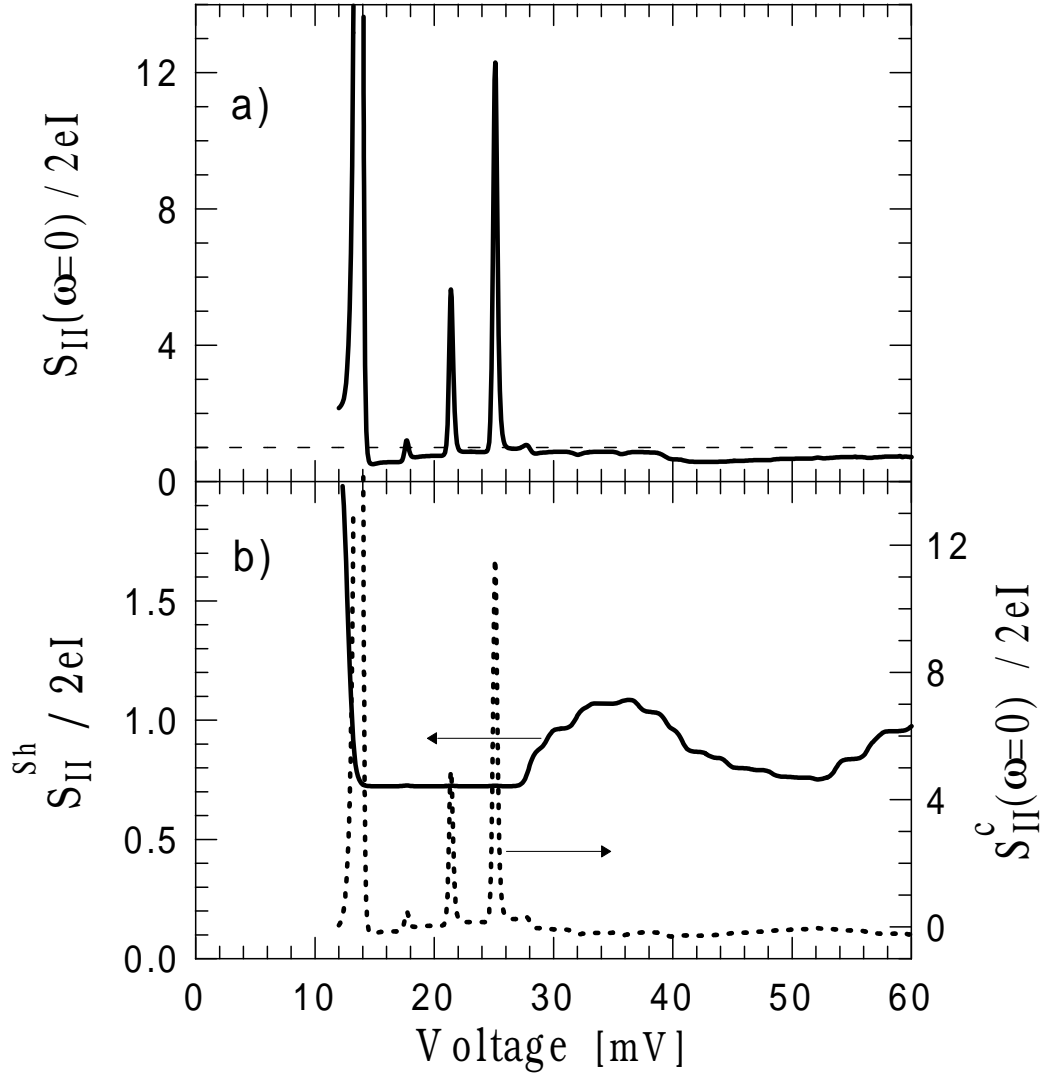


FIG. 12. Voltage dependence of the zero-frequency current shot noise (a) in the system defined in Fig.10. In part (b) two components of the shot noise S_{II}^{Sh} (solid curve) and $S_{II}^c(\omega = 0)$ (dashed curve) are presented.

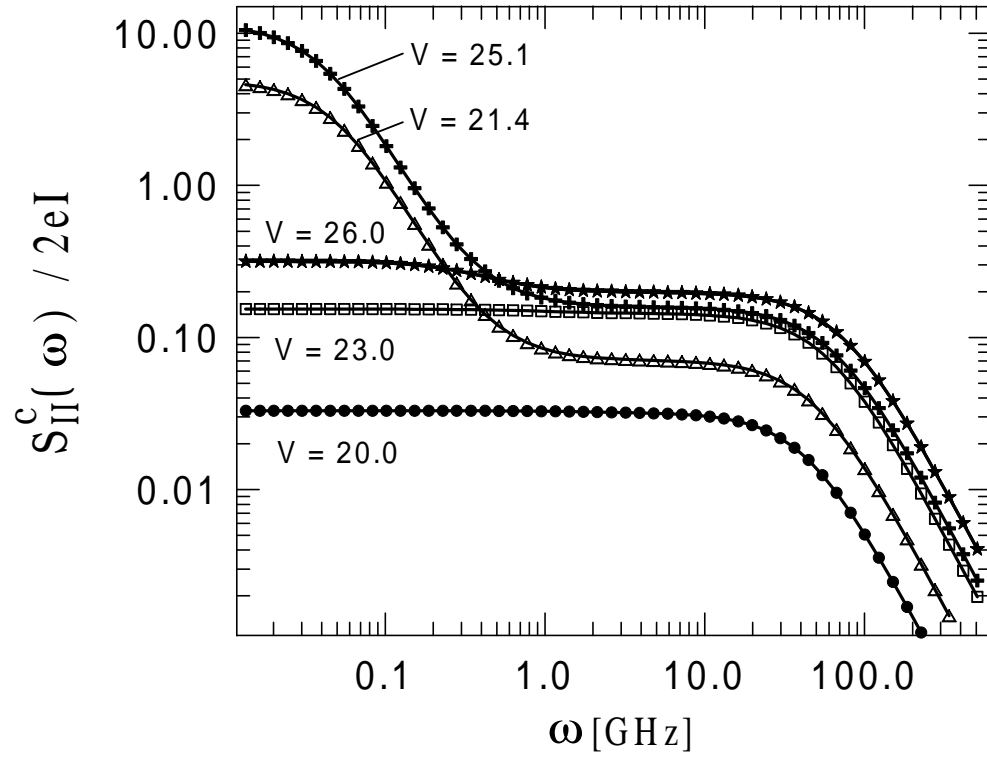


FIG. 13. Frequency dependence of the current noise $S_{II}^c(\omega)$ in the system as in Fig.10 for indicated voltages. The curves for $V = 21.4\text{mV}$ and $V = 25.1\text{mV}$ correspond to the maxima of the current shot noise seen in Fig.12 in the range of NDR.